

$D_{SS}, D_{LL}, D_{SL}, D_{LS},$ and P for $pp \rightarrow pp$ at 600 to 800 MeV

C. L. Hollas, D. J. Cremans, K. H. McNaughton, P. J. Riley, R. F. Rodebaugh, and Shen-wu Xu
University of Texas at Austin, Austin, Texas 78712

B. E. Bonner, M. W. McNaughton, H. Ohnuma,* O. B. van Dyck, and Sun Tsu-hsun†
Los Alamos National Laboratory, Los Alamos, New Mexico 87545

S. E. Turpin
Rice University, Houston, Texas 77251

B. Aas and G. S. Weston
University of California at Los Angeles, Los Angeles, California 90024
 (Received 11 June 1984)

We have measured the spin parameters $D_{SS}, D_{LS}, D_{SL}, D_{LL}$ ($K_{SS}, K_{LS}, K_{SL}, K_{LL}$), and P from 18° to 134° c.m. for $pp \rightarrow pp$ at 597, 647, 699, 750, and 800 MeV. (We also include four D_{NN} points that cross-check previous data.) The pp elastic phase shifts are now overdetermined near 597, 647, and 800 MeV and well determined near 699 and 750 MeV. The data are in satisfactory agreement with preexisting phase shift analyses and show no new energy dependence.

INTRODUCTION

The complete determination of the pp elastic amplitudes at 647 and 800 MeV has been a long-standing goal at LAMPF. In addition, interest in the energy dependence has been stimulated by the discovery of resonance-like structure at intermediate energies. Interpretations range from "dibaryon resonances" to threshold effects or effects from coupling to the major inelastic channels. The subject has been reviewed extensively.^{1,2}

Interpretation is hampered by inadequate energy-dependent data. Single-energy phase-shift solutions do not agree with (constrained) energy-dependent solutions, and although most agree on the existence of counterclockwise loops in the Argand diagrams for 1D_2 and 3F_3 , even this has been questioned.^{3,4} The structure for other partial waves ($^1G_4, ^3P_0$, etc.) is even less clear.

It has been shown⁵ that with the addition of the present data to the previously published data (summarized in Ref. 6), pp elastic amplitudes may be extracted at 647 and 800 MeV independently from the phase-shift analysis. Phase shifts and amplitudes are now overdetermined at 647 and 800 MeV. Similarly, at 600 MeV the present data add to and cross-check the overdetermined data set from SIN (Ref. 7) (near 580 MeV).

Near 699 and 750 MeV, the new data add to previously published measurements of D_{NN} (Ref. 8), A_{NN} (Ref. 9), A_{LL} (Ref. 10), and A_{SL} (Ref. 11) to give 11 spin parameters. [Since $D_{ij}(\theta) = K_{ij}(\pi - \theta)$, the present data give $P, D_{SS}, D_{LS}, D_{LL}, K_{SS}, K_{LS},$ and K_{LL} .] However, not all parameters are measured at the same energies or angles, so that a phase-shift analysis is required.

EXPERIMENTAL METHOD

In principle, the experimental method is similar to previous measurements^{12,13} except for the addition of a mag-

net to precess the final-state proton spin.

Briefly, the LAMPF polarized proton beam was precessed to one of the three standard¹⁴ spin directions $N, S,$ or L and focused onto a 7.5-cm-thick liquid-hydrogen target. The magnitude and direction of the beam polarization were monitored to $\pm 1\%$ and $\pm 0.5^\circ$, respectively, by a combination of the quench ratio and beam-line polarimeters in two adjacent beam lines.^{15,16}

Both elastically scattered protons were detected in multiwire drift chambers (MWDC's) allowing the use of angular correlations to reduce background to $\leq 1\%$. The magnet (Fig. 1) performed the two functions of a low-resolution spectrometer ($\Delta p/p \approx 1\%$) and precession of the final-state proton spin through 90° .

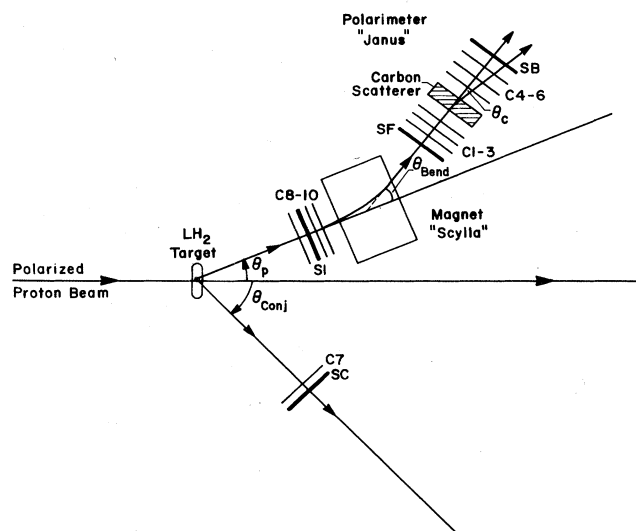


FIG. 1. Experimental layout. C1–C10 are multiwire chambers; S1, etc., are scintillators.

For D_{SS} and D_{LS} measurements the magnet was turned off and the carbon polarimeter [JANUS (Ref. 17)] measured the final-state S spin directly. For D_{LL} and D_{SL} the magnet bend θ_B was set for a precession angle $\theta_{pre}=90^\circ\pm 1^\circ$. The precise bend angle was measured to $\pm 0.2^\circ$ for every event by MWDC's before and after the magnet and the mean precession angle deduced ($\theta_{pre}=1.793\gamma\theta_B$). A check on the precession was made by comparing the measured bend with that deduced from the magnet shunt current and the magnetic field map. We conclude that both initial- and final-state spin directions were known to $\pm 0.5^\circ$ and, therefore, contribute a negligible uncertainty to the final result.

The final results for D_{ij} ($i, j=S$ or L) are given by measured asymmetries divided by beam polarization and carbon analyzing power, after correction for small unwanted spin components. Flipping the beam spin every two minutes canceled instrumental asymmetries. The carbon analyzing power was taken from a global fit¹⁸ updated to include recent data¹⁹ and has an uncertainty $\Delta A_c = \pm 2\%$ from 150 to 800 MeV. The final uncertainty is dominated by counting statistics, with ΔA_c included (in quadrature) for every point. Overall normalization is $\pm 1\%$ (Refs. 15 and 16), common to all previous data from LAMPF, and has not been included. This normalization should be applied equally to all spin parameters (D_{ij} , K_{ij} , and A_{ij}) from LAMPF.

Instrumental asymmetries do not cancel from the measurement of the polarization parameter P . The following checks on instrumental asymmetries were therefore made: (1) comparison with previous data for P near 40° c.m. (Ref. 16); (2) comparison of data at c.m. angles θ and

$(180-\theta)$; (3) comparison of P with zero at $\theta_{c.m.}=90^\circ$. With the magnet off, instrumental asymmetries were found to be small, with $e \leq 0.003$ (contributing an uncertainty e/A_c to P , where $0.25 \lesssim A_c \lesssim 0.5$). With the magnet on, however, the left-right instrumental asymmetry was $e \approx 0.01$, caused by the fringe field of the magnet, which caused unscattered tracks to appear to deflect by 0.02° .

Instrumental asymmetries were estimated and corrected for. The quoted data are dominated by magnet-off data, so the typical correction was $\Delta P \approx -0.01 \pm 0.003$. [This correction cancels to first order when data for θ and $(180-\theta)$ are combined.] The final uncertainty is dominated by counting statistics. Small contributions from uncertainties in carbon analyzing power and from the instrumental asymmetry are included in the tables.

Data are averaged over the full $\pm 2^\circ$ lab acceptance of the apparatus. The mean scattering angle was measured for each case to $\pm 0.15^\circ$ lab. The present data supersede the data presented at the 1983 Karlsruhe conference.²⁰ Further details are contained in two theses.^{19,21}

We also include four D_{NN} points, which duplicate previous data.¹² The 30° lab point was taken as a cross check. The 10° , 16° , and 23° lab points were a by-product of an experiment (in progress) to measure spin transfer in $pp \rightarrow pn\pi$. The method used was essentially identical to that used previously.¹² (Since the magnetic field was vertical, it had no effect on the N spin. The 30° point used both magnet and conjugate detector to eliminate background; the 10° , 16° , and 23° points used only the magnet.) The D_{NN} data are in good agreement with previous data and in fair agreement with Arndt's²² phase-shift fits.

TABLE I. Spin parameters D_{LL} and D_{SL} for $pp \rightarrow pp$ at 800 and 647 MeV.

θ_{lab}	$\theta_{c.m.}$	D_{LL}	ΔD_{LL}	D_{SL}	ΔD_{SL}
pp \rightarrow pp 800 MeV					
7.9	18.8	0.802	0.029	-0.032	0.030
14.7	34.8	0.638	0.020	-0.202	0.017
19.6	46.2	0.536	0.021		
22.2	52.0			-0.336	0.017
24.8	57.8	0.424	0.021	-0.343	0.017
29.8	68.8	0.291	0.023	-0.380	0.016
34.8	79.4	0.247	0.018	-0.374	0.014
40.0	90.0	0.260	0.014	-0.394	0.014
45.1	100.2	0.280	0.017	-0.447	0.016
50.6	111.0	0.235	0.015	-0.439	0.014
56.6	122.1	0.198	0.020	-0.430	0.015
62.6	133.1	0.117	0.049	-0.355	0.076
pp \rightarrow pp 647 MeV					
7.7	17.8	0.777	0.046	0.036	0.054
14.8	34.1	0.656	0.022	-0.193	0.021
19.9	45.5	0.582	0.021	-0.361	0.020
25.0	56.8	0.517	0.020	-0.446	0.020
29.8	67.2	0.453	0.018	-0.466	0.019
34.7	77.5	0.405	0.018	-0.449	0.019
40.6	89.7	0.254	0.026	-0.354	0.018
46.3	101.0	0.122	0.016	-0.275	0.016
52.0	112.0	0.060	0.022	-0.301	0.024
57.7	122.8	0.031	0.039	-0.227	0.065

Similarly, the new data for P at 647 and 800 MeV are in agreement with (and much less precise than) previous data.^{16,23,24} We include two values in Table IV which extend the angular coverage and agree well with the phase-shift predictions.

CONCLUSION

The data are presented in the tables (using the Ann Arbor convention,¹⁴ with all spins being measured in the laboratory frame) and in Fig. 2 in comparison with Arndt's²² phase-shift fit SP84. Previous data (Refs. 12, 13, 15, 16, 23, and 24) are included in Fig. 2 for comparison where appropriate. Recent data from SIN (Refs. 25 and 26) near 580 MeV are not shown, but agreement is good both with the present data and the phase-shift fit.

In general, the fits of phase shifts to data are fair (Fig. 2), and no surprising or new structure is observed. We are somewhat surprised, however, that the fits are not better. For example, the structure in D_{LS} near 110° c.m. at 750 MeV looks like a precursor of the similar 800-MeV structure, but is poorly represented by the fit. Similarly, the knee in D_{LL} at 90° c.m. is under-represented at 750 (and perhaps 700) MeV. At 800 MeV the data set spans 12 spin-dependent parameters and is sufficient to completely determine the $I=1$ phase shifts, but the fit (SP84) has $\chi^2=36$ for 11 D_{LL} points and $\chi^2=32$ for 11 D_{SL} points. Arndt's single-energy solution (C800) fits D_{LL} quite well ($\chi^2=11$ for 11 points) and fits D_{SL} better at most angles, but is worse near 70° c.m. (with total $\chi^2=32$ still).

The obvious conclusion is that the global data set contains systematic errors beyond the quoted uncertainties.

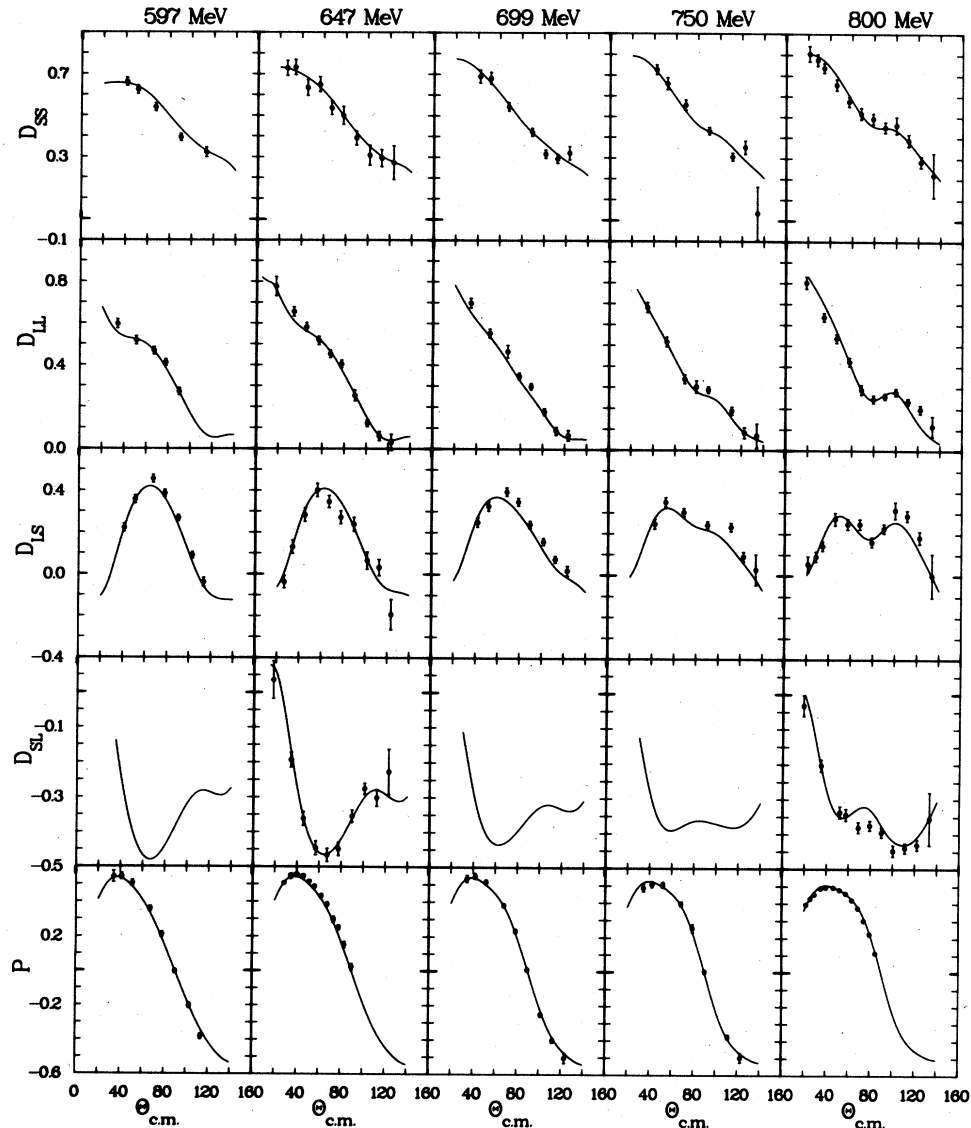


FIG. 2. Data in comparison with Arndt's phase-shift fit SP84. Previous data from Refs. 12, 13, 15, 16, 23, and 24 have been included where appropriate.

TABLE II. Spin parameters P , D_{SS} , D_{LS} , and D_{LL} for $pp \rightarrow pp$ at 750, 699, and 597 MeV.

θ_{lab}	$\theta_{c.m.}$	P	ΔP	D_{SS}	ΔD_{SS}	D_{LS}	ΔD_{LS}	D_{LL}	ΔD_{LL}
pp \rightarrow pp 750 MeV									
14.8	34.6	0.488	0.021					0.681	0.024
18.1	42.3	0.508	0.016	0.727	0.023	0.246	0.023		
22.5	52.1	0.506	0.016	0.660	0.029	0.351	0.022	0.517	0.023
30.0	68.6	0.396	0.013	0.557	0.025	0.302	0.020	0.339	0.021
35.0	79.2	0.256	0.023					0.303	0.029
40.2	90.1	0.003	0.010	0.432	0.018	0.241	0.018	0.288	0.015
51.0	111.3	-0.376	0.012	0.308	0.019	0.232	0.019	0.188	0.019
57.2	122.8	-0.498	0.026	0.353	0.032	0.090	0.023	0.084	0.026
63.3	134.0			0.035	0.128	0.028	0.073	0.070	0.058
pp \rightarrow pp 699 MeV									
14.9	34.6	0.535	0.020					0.698	0.023
18.1	41.9	0.550	0.016	0.690	0.031	0.249	0.022		
22.5	51.8	0.517	0.012	0.682	0.028	0.326	0.022	0.553	0.021
30.0	68.1	0.382	0.010	0.544	0.020	0.395	0.020	0.466	0.030
35.0	78.7	0.235	0.011			0.347	0.018	0.348	0.016
40.2	89.4	0.010	0.009	0.422	0.019	0.240	0.017	0.299	0.015
46.3	101.6	-0.251	0.011	0.317	0.020	0.158	0.017	0.179	0.016
51.9	112.4	-0.402	0.012	0.294	0.021	0.074	0.016	0.088	0.019
57.7	123.3	-0.504	0.029	0.322	0.032	0.019	0.024	0.067	0.025
pp \rightarrow pp 597 MeV									
14.9	34.1	0.542	0.033					0.596	0.022
18.1	41.2	0.544	0.018	0.662	0.020	0.221	0.019		
22.6	51.0	0.505	0.017	0.624	0.020	0.357	0.019	0.517	0.020
30.0	67.2	0.358	0.014	0.539	0.019	0.455	0.018	0.467	0.018
35.1	77.8	0.211	0.015			0.386	0.017	0.411	0.016
41.1	90.1	-0.005	0.011	0.394	0.017	0.268	0.015	0.272	0.017
47.6	103.0	-0.203	0.015			0.090	0.016		
53.0	113.4	-0.383	0.016	0.322	0.023	-0.038	0.021		

(The global data set has a total $\chi^2=1469$ for 692 points near 800 MeV.) In this light, the quoted uncertainties for this fit must be treated with caution. For example, at 70° c.m., 800 MeV, we have $D_{SL} = -0.313 \pm 0.005$ for the C800 fit, $D_{SL} = -0.380 \pm 0.016$ for the data.

An internal consistency check is possible among the spin-transfer data. Transforming the spins to the center of mass (and using lower case subscripts for c.m. spins),

$$D_{sl} = D_{SS} \sin \theta_{lab} + D_{SL} \cos \theta_{lab} \\ = -(D_{LS} \cos \theta_{lab} - D_{LL} \sin \theta_{lab}) = -D_{ls} .$$

D_{sl} and D_{ls} are plotted in Fig. 3 showing that the data are, indeed, internally consistent. If D_{LL} and D_{SS} are

TABLE III. The spin parameter D_{NN} for $pp \rightarrow pp$ at 800 MeV.

θ_{lab}	$\theta_{c.m.}$	D_{NN}	ΔD_{NN}
10.0	23.8	0.828	0.043
16.4	38.8	0.852	0.029
23.4	54.7	0.797	0.026
30.0	69.2	0.768	0.033

correct, then $D_{SL} + D_{LS}$ must be ≈ -0.14 so that the poor fits for D_{SL} and D_{LS} at 70° c.m. are related.

From the data: $D_{LS} + D_{SL} = 0.248 - 0.380 = -0.132$.

From the fit: $D_{LS} + D_{SL} = 0.172 - 0.313 = -0.141$.

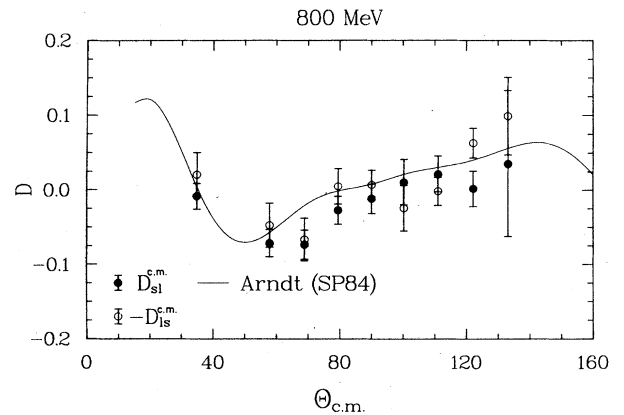


FIG. 3. D_{sl} and $-D_{ls}$ (c.m.) at 800 MeV. $D_{sl} = -D_{ls}$ demonstrates internal consistency (see the text).

Similarly at 80° c.m., the low D_{SL} point is related to the high D_{SS} point, etc.

The experimental methods are closely similar for D_{SL} and D_{LL} (this paper) and for D_{LS} and D_{SS} (Ref. 12), and fairly similar for this paper compared with Ref. 12. We cannot conceive of any systematic error which could make D_{LS} 0.07 lower, D_{SL} 0.07 higher, and leave D_{SS} and D_{LL} unchanged at 70° ; or, make D_{SS} lower, D_{SL} higher, and leave D_{LS} and D_{LL} unchanged at 80° , as would be required to agree with the phase-shift fits.

TABLE IV. The polarization parameter P for $pp \rightarrow pp$ at 647 MeV.

θ_{lab}	$\theta_{\text{c.m.}}$	P	ΔP
7.7	17.8	0.352	0.037
10.6	24.4	0.429	0.036

This work was supported by the U.S. Department of Energy.

*Present address: Tokyo Institute of Technology, Oh-Okayama, Tokyo 152, Japan.

†On leave from Institute of Atomic Energy, Academia Sinica, Peking, People's Republic of China.

¹A. B. Wicklund, in *High Energy Spin Physics—1982*, Proceedings of the Fifth High Energy Spin Symposium, AIP Conf. Proc. No. 95, edited by G. Bunce (AIP, New York, 1983), p. 168.

²M. P. Locher, in *Proceedings of the Tenth International Conference on Few Body Problems in Physics, Karlsruhe, Germany, 1983*, edited by B. Zeitnitz (American Elsevier, New York, 1984).

³F. Lehar, see Ref. 1, p. 191.

⁴J. Bystricky *et al.*, Saclay Report No. DPhPe 82-09, 1982.

⁵R. F. Rodebaugh and B. E. Bonner, see Ref. 2, Vol. II., p. 43.

⁶M. W. McNaughton, see Ref. 1, p. 243.

⁷E. Aprile *et al.*, see Ref. 1, p. 246.

⁸C. L. Hollas *et al.*, Los Alamos National Laboratory Report LA-UR-83-3048, 1983, submitted to Phys. Lett.

⁹T. S. Bhatia *et al.*, Phys. Rev. Lett. **49**, 1135 (1982).

¹⁰I. P. Auer *et al.*, Phys. Rev. Lett. **41**, 1436 (1978).

¹¹I. P. Auer *et al.*, Phys. Rev. Lett. **51**, 1411 (1983).

¹²M. W. McNaughton *et al.*, Phys. Rev. C **25**, 1967 (1982).

¹³M. W. McNaughton *et al.*, Phys. Rev. C **26**, 249 (1982).

¹⁴*Higher Energy Polarized Beams (Ann Arbor, 1977)*, Proceedings of the Workshop on Higher Energy Polarized Proton Beams, AIP Conf. Proc. No. 42, edited by A. D. Kirsch and A. J. Salthouse, AIP, New York, 1978), p. 142.

¹⁵M. W. McNaughton *et al.*, Phys. Rev. C **23**, 1128 (1981).

¹⁶M. W. McNaughton and E. P. Chamberlin, Phys. Rev. C **24**, 1778 (1981).

¹⁷R. D. Ransome *et al.*, Nucl. Instrum. **201**, 309 (1982).

¹⁸R. D. Ransome *et al.*, Nucl. Instrum. **201**, 315 (1982).

¹⁹D. J. Cremans, M. S. thesis, University of Texas, 1983.

²⁰D. J. Cremans *et al.*, see Ref. 2, Vol. II., p. 21.

²¹R. Rodebaugh, M. S. thesis, University of Texas, 1984.

²²R. Arndt *et al.*, Phys. Rev. D **28**, 97 (1983).

²³P. Bevington *et al.*, Phys. Rev. Lett. **41**, 384 (1978).

²⁴M. W. McNaughton *et al.*, Phys. Rev. C **25**, 2107 (1982).

²⁵D. Besset *et al.*, Phys. Rev. D **21**, 580 (1980).

²⁶E. Aprile *et al.*, Phys. Rev. D **27**, 2600 (1983).